Journal of Materials and Engineering Structures

Review Paper

Role of Excessive Iron on Hyper-Eutectic Al-Si Automotive Alloy: A Review

Mohammad Salim Kaiser

Directorate of Advisory, Extension and Research Services, Bangladesh University of Engineering and Technology, Dhaka-1000, Bangladesh

ARTICLE INFO

Article history :

Received : 30 October 2020

Accepted : 15 January 2021

Keywords:

Al-Si alloy

Age hardening

Mechanical properties

Wear and Corrosion

ABSTRACT

Aluminum alloys always content the element iron more or less as a common impurity. It is unavoidable and has undesirable effects to ductility and cast ability, mainly in cast Al-Si alloys. The quantity of Fe content as well has a significant effect on the mechanical properties of the Al-Si alloys. Heat treatment may also affect the different properties of these alloys. Hypereutectic alloys which contents more than 12% Si are attractive candidates for automotive applications. It is well known that the excellent properties of hyper eutectic aluminium alloy are based on the primary Si particles as distributed in the matrix. Experiments in this regards have been carried out on physical, mechanical, thermal etc. behavior of these alloys by a good number of researcher. This article presents a literature review on the early investigated role of excessive iron on the different properties of hyper-eutectic Al-Si automotive alloy. In addition, the main factors which affect its mechanism are scheduled.

1 Introduction

Al-Si alloys are one of the striking materials in automotive industry among most commonly used aluminum alloys [1-3]. Silicon advances the strength of these alloys by the formation of hard Si phase into the Al matrix. More than 12% Si content into this alloys termed as hypereutectic alloys which surround normally primary silicon phase in the eutectic matrix. The presence of coarse plate-like nature of the Si phase into cast eutectic alloys initiates to crack and fracture under load. These types of phases decrease the ductility of the alloys [4, 5].

In addition the different properties as physical, mechanical, thermal etc. of these alloys depend on the Cu, Mg, Ni and Fe-content as well as the nature of silicon particles. Many compound intermetallic phases are formed with these types of

* *Corresponding author. Tel.: +88-966312900.*
E-mail address: mskaiser@iat.buet.ac.bd

e-ISSN: 2170-127X,

RESEARCH REVIEW of Sciences and Technologies

elements in the Al-Si alloys during casting and heat treatment [6-8]. Aluminum alloys always contents more or less iron as a common impurity that take place from a number of possible sources during casting. It has to be well-known that iron always does not exercise a negative influence on the properties of the alloys. Sometimes alloying addition improves the processing capabilities and strength of the alloys. Amount of Fe organize the intermetallic phases like Al_3Fe and Al_6Fe but when Si is present in to the alloys the dominant phases are α-phase Al_8Fe_2Si and β-phase Al_5FeSi. It is well documented that a surplus amount of iron in Al-Si casting alloys can lead to the formation of the β phase Al_5FeSi intermetallic with monoclinic crystal structure. These needles like phases precipitate in the interdendritic along with intergranular regions which are more unwanted. The mechanical properties, particularly ductility are unfavorably affected by such type of needles like particles [9, 10].

In recent years there has been done a lot of research work to explore the effect of various elements on the mechanical properties of Al-Si alloys [11-13]. Though, there is no systematic work has been conducted to investigate the role of excessive iron on the different properties of Al-Si alloys. In this paper, an effort has been made to review the effects of excessive iron on the different properties of automotive alloys like hyper-eutectic Al-Si and to provide a superlative choice of material for supplementary on-going research.

2 Processed material

Investigated hyper-eutectic Al-Si alloys were prepared by remelting the aluminum engine block in a resistance furnace and the full chemical composition of Alloy 1 (0.795% Fe) and Alloy 2 (5.910% Fe) showing the contents elements of Si, Ni, Cu, Mg, Zn, Mn, Ti are stated elsewhere [14-16]. For ageing treatment the cast alloys were homogenized at 400°C for a time period of 18 hours. Solutionized treatment also was done at 530°C for 2 hours followed by quenching into the salt ice water. Vickers hardness testing machine was used to measure the microhardness and Type 979 meter was used for electrical conductivity measurement of the materials. The Wiedemann–Franz law was used for calculating the thermal conductivity from those electrical conductivity data [17]. Tensile and impact test were carried out according to ASTM specification. Optical and Scanning Electron Microscope investigation were carried out in usual way [14]. The wear properties along with the frictional behaviors of the investigated alloys were examined following ASTM standard G99-05 with the help of a pin-on disc type apparatus [15]. The test of corrosion behavior at different environments was performed using conventional gravimetric measurements [16]. Solutions of pH1 and pH13 environment were prepared by adding HCl and NaOH respectively.

3 Review on properties

3.1 Age-hardening behavior

The age hardening and precipitation behavior of hyper-eutectic Al-Si automotive alloy were carried out by Kaiser et al where the influence of Fe was studied in details [14]. When the cast hyper-eutectic Al-Si automotive Alloy 1 and excessive Fe added Alloy 2 were aged for a constant time 60 minutes at different temperature, there a phenomenon of an age-hardening was observed for both the alloys as reported earlier [8, 18]. The experimental results of isochronal ageing are plotted in Fig. 1a. However, following the first one another hardness peak was observed with a decrease at intermediate stage in age hardening curves. In the ageing process at initial stage fine and profuse GP zones distribute in the matrix homogeneously causes the significant strengthening effects. Conversely at the midway stage of aging the metastable phases was formed and kept semi-coherence with the matrix. As a result dislocation movement are effectively resisted, therefore have positive strengthening effect [19]. In opposition, these GP zones extremely dissolved before formation of the metastable phase in precipitation sequence of the alloys accordingly showed the inferior effect of age-hardening. At higher ageing temperature both the alloys attain a sharp decrease in hardness due to precipitates coarsening and recrystallization. Excessive Fe added alloy did not show addition ageing response. The higher amount of Fe formed different iron reach intermetallic like Al_3Fe, α-Al_8Fe_2Si, β-Al_5FeSi, δ-Al_4FeSi_2 and γ-Al_3FeSi during solidification causes the higher hardness of the alloys, specially for β-Al_5FeSi [20].

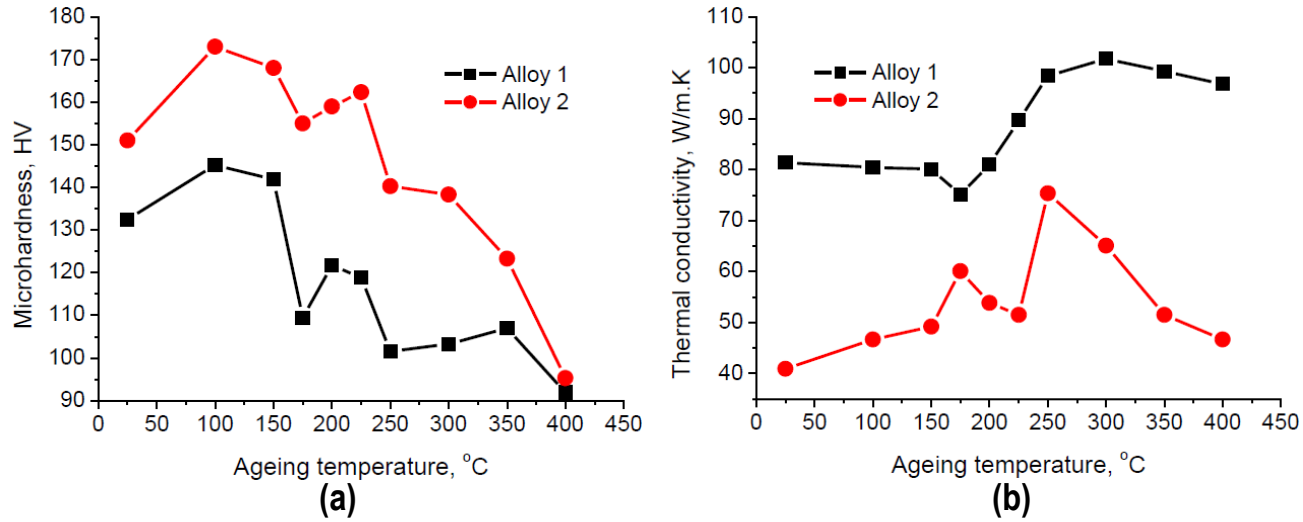

Fig. 1 – Variation of (a) microhardness and (b) thermal conductivity of the alloys as a function of the isochronal ageing duration for 1 hour

From the same research it was showed that the tiny number in thermal conductivity increases at initial stage of ageing [14]. It is because of stress relieving behavior of the alloys (Fig. 1. b). The major increase in conductivity is due to dissolve of GP zones before metastable phase formation. This results a going up in conductivity. The subsequent decrease in conductivity is due fine precipitates created by the elements into the alloys. Following the steep up in conductivity is considered to recovery of strain as well as dissolution of metastable phases of the alloys. The thermal conductivity of Fe added alloy shows lower due to higher concentration of elements in the solid solution [21]. At higher temperature of ageing different Fe associated intermetallics were formed which was responsible for extra reduction of conductivity of this alloy.

Kaiser et al also studded the isothermal ageing behavior of these cast alloys for different time at selected temperature of 175 and 200°C (Fig. 2a and 2b) [14]. Both the alloys due to ageing attain the double aging peaks and achieve the higher strength. In the course of ageing, formation of GP zones and metastable phases are able to successfully strengthen the alloys and direct to the condition of peak aged. In the juncture of GP zones to metastable phases the inferior age hardening effect are shown of alloys. At this ageing stage through dissolution the quantity of GP zones decreases continually and the metastable phase has not grown up fully as a result the minimum efficiency to resist the dislocation movement. For that reason, such aging values are observed of the alloys in between two aging peaks. Finally the decreasing of microhardness occurs due to over ageing effect and coarsening of fine precipitates [12]. The double ageing peaks at lower temperature for all the alloys are prominent. At the higher ageing temperature formation of GP zones, dissolution of GP zones, formation of metastable phase and grain coarsening occurs earlier. From the figures it is clear that the peak hardness is achieved when the alloys are isothermally aged for a prolong time of 240 minutes at 175°C temperature.

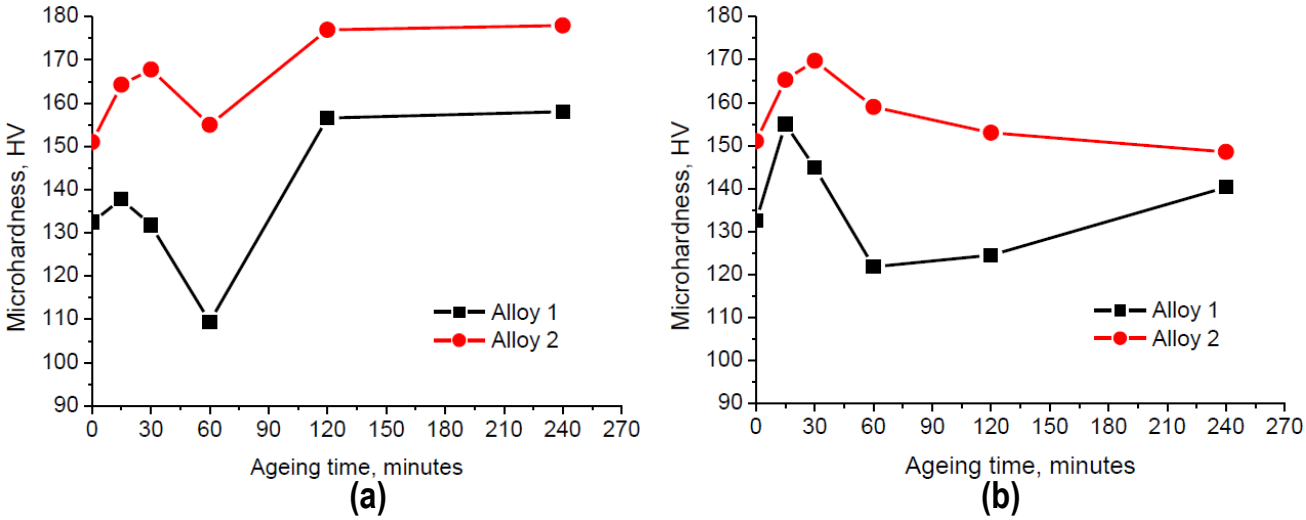

Fig. 2 – Variation of microhardness of the alloys as a function of isothermal ageing at (a) 175°C and (b) 200°C

A thorough characterization on the microstructures of the hyper-eutectic Al-Si automotive alloy was carried out by Kaiser et al [14]. The role of Fe on the microstructure also studied as displayed in Fig. 3. A typical structure was observed in the optical micrograph of the Al-Si Alloy 1 where both primary blocky and eutectic plate-like Si phases accumulated in the aluminum matrix (Fig. 3a). The presence of higher amount of Fe since it formed different intermetallic compounds with the β-Al_5FeSi intermetallic phase in a plate-like morphology. Figure 3b exhibits some β-Al_5FeSi intermetallics in Alloy 2 with high concentration of Fe and without any modifiers. When the alloys were gone through the ageing process for the time ranging of 60 minutes at temperature of 350°C, it was appeared to be almost fully recrystallized state (Fig. 3c and 3d). This level of temperature recrystallization of these alloys took place as a result the dendritic pattern was removed and the precipitation coarsening occurred in to the microstructure. The microstructure also consisted of equi-axed grains as the second phase constituents segregated into the alloys at the grain boundaries [18]. β-Al_5FeSi phases are almost absent into the microstructure of Al-Si alloy but the needle-like β-Al_5FeSi platelets are visible in the matrix of Fe added alloy because of this temperature does not dissolve this type of phases.

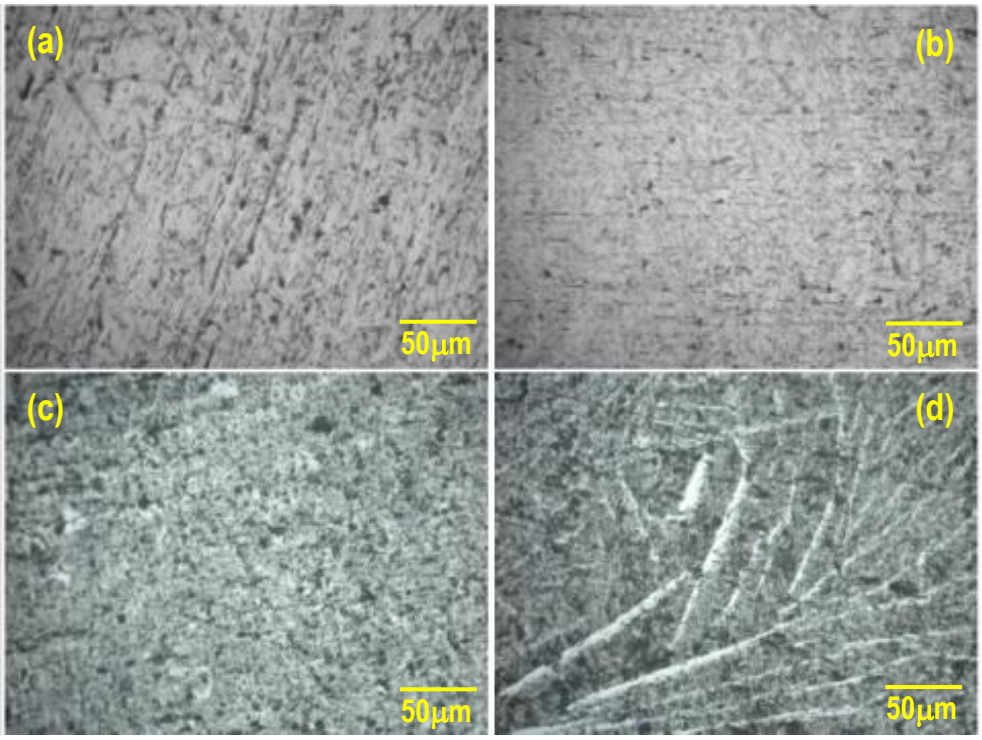

Fig. 3 – Optical micrograph of as cast solution-treated at 530ºC for 2h (a) Alloy 1, (b) Alloy 2 and after ageing treatment for 60 minutes at 350°C (c) Alloy 1, (d) Alloy 2

3.2 Mechanical Properties

The influence of iron on the mechanical properties such as ultimate tensile strength, percentage elongation and impact energy at peak aged conditions of the alloys has been studied extensively by Kaiser et al [14]. When aged at 175°C for 240 minutes both the alloys attained the peak aged condition. While Fe remain in to the Al-Si-based alloy there is a tendency to form the common needle-like β-Al_5FeSi intermetallic phases and increases the concentration of the intermetallics with Fe content. Their company strongly degrade these properties of the Alloy 2. It is well established that the Fe containing intermetallics are very brittle and hard compounds. They strongly proceed as stress raisers and points of weakness. As a result reduce the strength and ductility through to macro-cracks of the alloys. They exist as discrete particles with highly faceted nature which has relatively low bonding strength among alloy matrix causes the degradation of impact energy [22]. From the Fig. 4 it can be found that the base Alloy 1 shows the higher strength, elongation and impact energy at peak aged conditions.

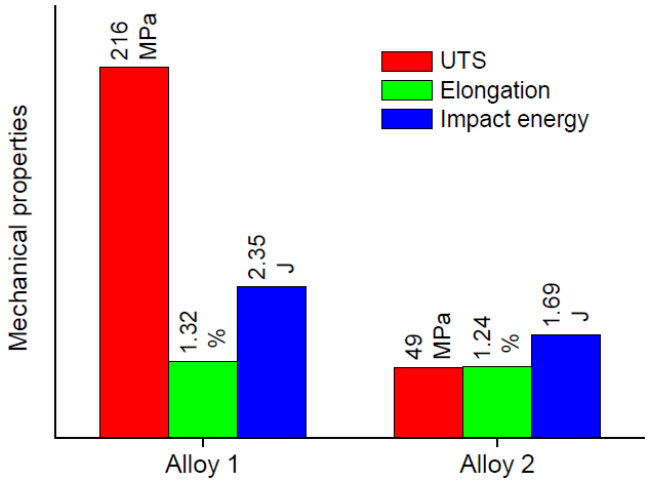

Fig. 4 – Mechanical properties of both the alloys at peak aged condition

They also worked on the fracture behavior of the peak aged alloys when the tensile samples were tested under strain rate of $10^{-3}s^{-1}$ [14]. The SEM fractographs of the Al-Si Alloy 1 show the signs of a certain amount typical intergranular cleavage fracture with the creation of secondary cracks (Fig. 5a). Some dimple morphology with ductile α-phase fracture is observed which indicate a mixed fracture. The figure also demonstrated that the plane of the fracture dependent on the orientation of the grain and interdendritically eutectic Si. In general mode of fracture observed in Fig. 5b the SEM fractograph of Fe added Alloy 2 exhibits more crack propagation offered by the massive cleavage of the brittle and needle-like shape Fe rich intermetallics. Since the Fe content increased into the alloys, a large amount of these Fe rich β-platelets is expected which spread the cracks. The quantity of cleavage facets also augmented into fracture surfaces. So the cracks initiations to a large extend were observed due to outsized the plate-like β-Al_5FeSi phase from the surface compared to the Si particles [23].

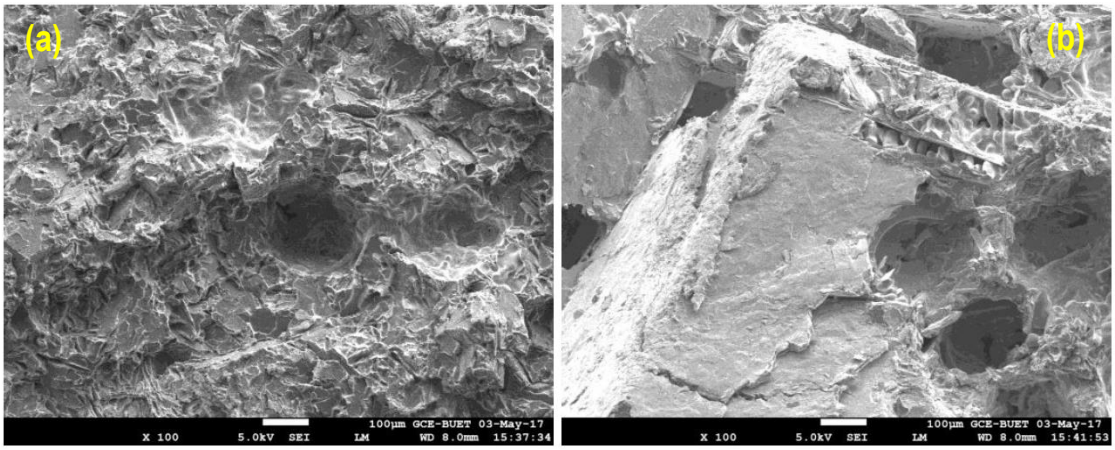

Fig. 5 – SEM fracture surfaces of (a) Alloy 1 and (b) Alloy 2 at peak aged condition 175°C for 240 minutes

3.3 Wear behaviour

Detailed studies of the influence of Fe on the wear behavior were carried out on hyper-eutectic Al-Si automotive alloy [15]. The wear rate and friction coefficient were measured at different sliding distance under constant pressure and velocity of 1.0MPa (Load = 20N) and 0.64 ms^{-1} respectively. The plotted results are displayed in Fig.6. It evidently makes known wear resistance decreases with the increases of sliding distance for both the alloys. The wear rate increasing can be credited to long-lasting intimate get in touch between the two contact surfaces. The fragmented intermetallics also weaken the tribolayer and make easy the progress of the instigation and spread of microcracks. Alloy 2 contents the higher volume fraction and aspect ratio of intermetallics. The negative effects of β-phase increased with their size and volume fraction of Alloy 2 and, therefore, Alloy 1 exhibited better wear behavior (Fig. 6a)[24].

From the Fig. 6b it can be noticed that the coefficient of friction increase sharply during the initial stage of sliding distance and afterword reaches a steady state condition. This nature of friction coefficient is due to uneven contact between specimen pin and the counterpart disc. When achieved the ideal contact, the coefficient shows almost steady state value. Alloy 2 resistant through the hard β-Al_5FeSi particles, exhibit higher friction coefficient than that of Alloy 1. Fe also forms different fine precipitates which also responsible for higher wear resistance values [25].

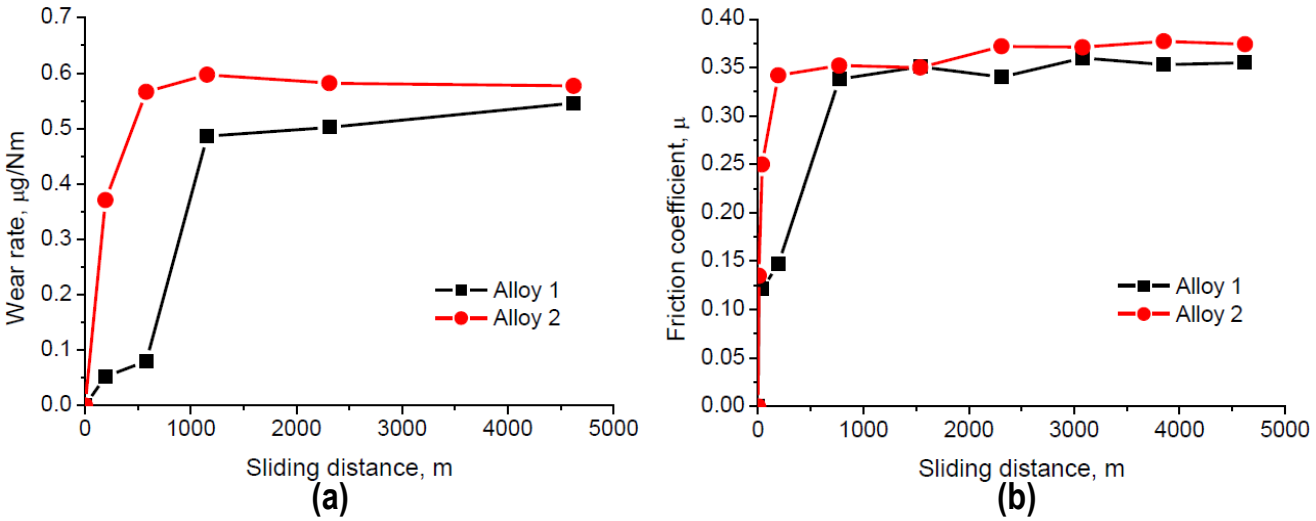

Fig. 6 – Variation of (a) wear rate and (b) friction coefficient of the alloys as a function of sliding distance at applied pressure and velocity of 1.0MPa (Load = 20N) and 0.64 ms^{-1} respectively

The influence of Fe on the worn surfaces after wear test of the experimental alloy was studied in detail [15]. Along with the sliding direction the long parallel grooves are undoubtedly evident on the surfaces for both the alloys. Abrasion of entrapped particles is the major foundation for this phenomenon. Figure 7a contents the SEM microphotograph of worn surface of Alloy 1. It exposed small cracks with grooves and dislodging of material those clearly indicating the nature of combination of abrasive and delaminative wear. Alloy 2 contents the higher volume fraction of needles like and coarser Fe-based intermetallics which initiate the failure of matrix and therefore resulted in a worn surface with subsurface cracks and large facets (Fig. 7b). These are indicated the nature of smaller ductile fracture. As the Fe rich alloys contents the higher number of β-platelets with different length and thickness which plays a negative role in the worn surface that confirmed the high wear rate [26]. Occasionally the inclusion of two cross β-platelets form cavities in to the matrix which increase the micro-pores and results the higher subfractures on the surfaces.

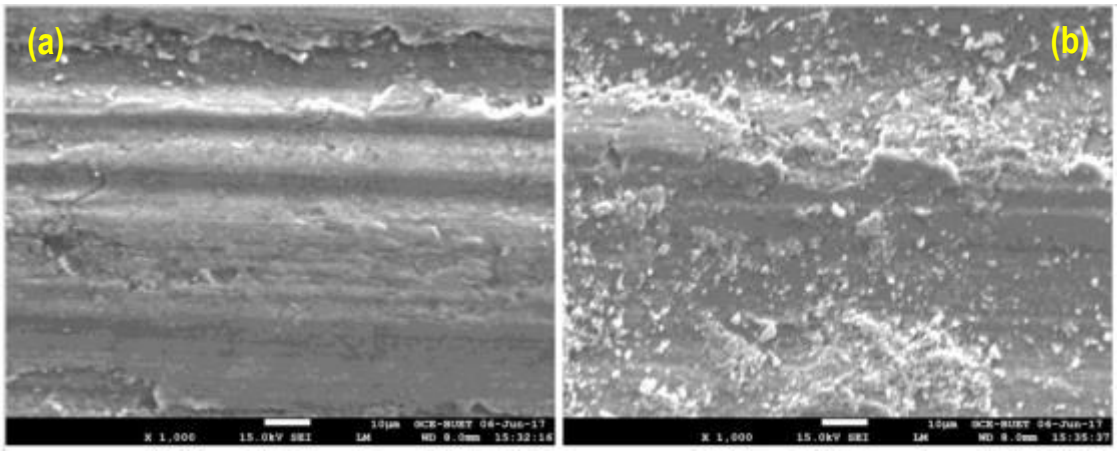

Fig. 7 – SEM micrographs of worn out surfaces after wear for 4600m (a) Alloy 1 and (b) Alloy 2 at applied pressure and velocity of 1.0MPa (Load = 20N) and 0.64 ms^{-1}respectively.

3.4 Corrosion behavior

Kaiser and Nur conducted a test on corrosion behavior of excessive Fe added Al-Si alloys [16]. They used different pH solutions exposed during 27 days. The results of corrosion rate in pH1 and pH13 environment are plotted in Fig. 8. Both the alloys maintained normal corrosion profiles by showing the initial steep rise in corrosion rate anticipation of a peak value. This was associated to the dynamic dissolution of the alloys surfaces. After that, the corrosion rate gradually declined due to devotion of oxide formation as well as passivity on the metal surface.

The maximum corrosion rate was observed at pH13 environment where the sodium hydroxide presence in the solution. The created oxide film on the surfaces was soluble in this solution as a result continuous degradation of the surfaces. Again in the pH1 environment where hydrochloric acidic presence in the solution, this provided hydrogen ions and accelerate the corrosion rate. These solution also content chloride ions which have an effect on the corrosion behaviour in a sense that increased chloride ions resulted the higher corrosion rate of the alloys [27]. Corrosion rate for both alloys as shown in Fig. 8a and 8b, increased quite abruptly within 3 days followed more or less constant values with some extend immersion time. After a long time of immersion corrosion products such as aluminum oxide and hydroxide make layer on the surface causes the lower corrosion rate. Then the uniform breaks down of these oxide and hydroxide maintain the constant corrosion rate. Aluminum performs as a very good corrosion resistance because it is very reactive and form quickly aluminum oxide at natural environment. Aluminum oxide create thin layer on the surface which avoid further corrosion. This film is reasonably steady in neutral as well as mildly acidic solutions, but dissolves rapidly in the higher pH of alkaline range. Alloy 1 supported the results by showing the lowest corrosion rate at pH1 and the highest at pH13. Fig. 8a associated the pH1 environment also suggested that corrosion rate was greater for Alloy 2 where the higher amount of iron was detrimental. Iron particles formed the intermetallics like Al_3Fe, more cathodic since hydrogen ions are ample to the Al matrix. Additionally, iron can sustain chemical reactions more efficiently than Al [28]. Figure 8b shows that at pH13 solution, Fe added Alloy 2 exhibited lower corrosion rates than Alloy 1. Fe-containing particles provide effective cathodes for reduction reactions thus enhancing the anodic dissolution of aluminium. Interestingly; it is also observed that the loss of aluminium and consequential surface enrichment of Fe leads to enhanced cathodic activity of the particles [29].

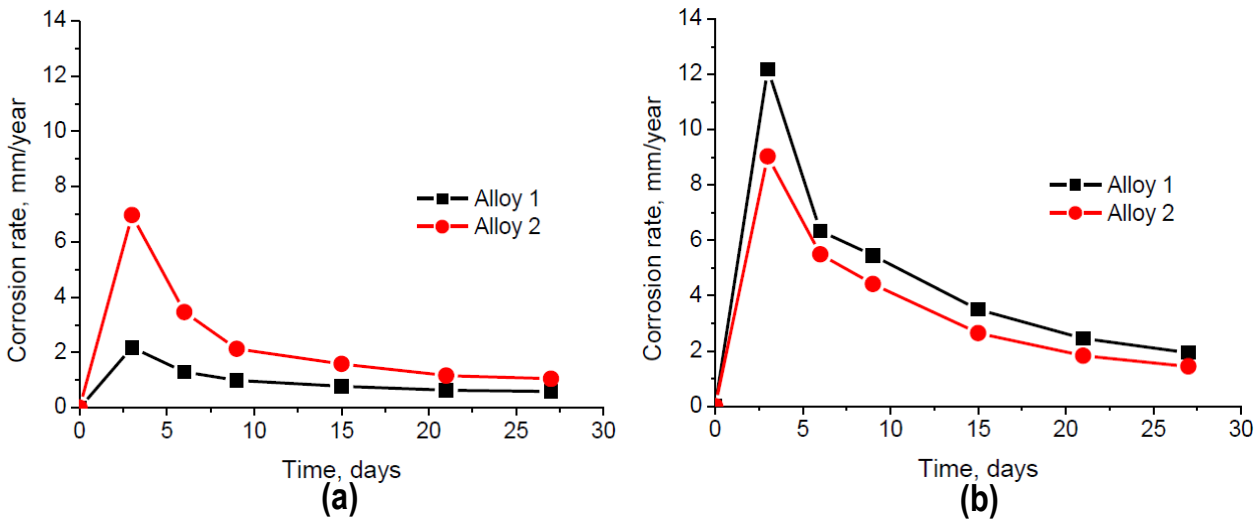

Fig. 8 – The change of corrosion rate for the experimental alloys at (a) pH1 and (b) pH13 environments as a function of immersion time

The microstructure of discussed Al-Si automotive alloys at peak aged condition characterized systematically by Kaiser and Nur [16]. Binary Al-Si alloy usually generate primary α-Al dendrites and eutectic Si into the aluminum matrix. When iron is supplemented at low level into this alloy a small amount of Fe-rich intermetallic phases are formed into the matrix. At the same time the eutectic Si particles comprise a platelets and acicular morphologies. There a number of void and cavities are accessible in the microstructure of the cast alloys (Fig. 9a). When the alloy contents higher level of Fe, it leads to formation of various intermetallic compounds like β-Al_5FeSi, Al_9FeSi_2, Al_3FeSi_2, Al_4FeSi_2 etc. in the microstructure. Comparatively higher number of void and cavities are also exposed into this alloy. These are created by higher level of the β-phase platelets which restrict the liquid flow during casting. While Alloy 2 consists of the excessive Fe compare to the Alloy 1 higher amount of Fe rich intermetallics as well as β-Al_5FeSi phase are shown in to the alloy (Fig. 9b) [30]. These are well documented in

the EDX analysis of the alloys. The corresponding EDX analysis by weight percent of the SEM confirms that Alloy 2 consists of higher weight amount of 7.18% Fe than Alloy 1 of 0.28% Fe. Alloy 1 contents 85.32% Al, 11.47% Si, 0.48% Ti, 0.34%Cr, 0.28% Fe, 0.72% Cu and 1.39% Zn and Alloy 2 contents 67.85% Al, 20.17% Si, 0.65% Cr, 0.55% Mn, 7.18% Fe, 1.05% Ni, 1.78% Cu and 0.76% Zn.

The SEM images of the corroded samples of both the alloys after 27 days methodically investigated by Kaiser and Nur as presented in Fig. 10 [16]. When the samples are immersed for prolong 27 days in pH1 medium external pits like spherical and narrow are visibly observed on the surfaces of alloys (Fig. 10a and 10b). The pitting like crystallographic cubic shaped is created due to corrosion in chlorides followed by uniform degradation of alloys. The chloride ions through the violent attack break down continually the passive film which is produced on the alloys surfaces during corrosion [27]. The alloys surfaces show the different types of pitting in terms of size, shape and intensity as different intermetallics at different amounts are present in the alloys. The elements were found by EDX analysis of the corresponding SEM of Alloy 1: weight percent of 60.46% O, 0.13% Na, 18.86% Al, 3.63% Si, 0.99% S, 0.19% Cl, 0.17% Ti, 0.56% Cr, 0.59% Ni, 0.83% Cu, 13.58% Br. Similarly the elements of Fe added Alloy 2 were: 60.13% O, 0.04% Na, 16.73% Al, 1.39% Si, 1.23% S, 4.18 % Cl, 0.26 % Cr, 0.44% Fe, 0.10% Ni, 0.50 % Cu, and 15.01% Br.

In case of pH13 solution immersed for same days, the alloys surfaces was covered with the corrosion product of black in nature and this layer became thicker due to concentration of higher NaOH (Fig. 10c and 10d). As a result in this alkaline solution, the corrosion layer appeared more packed together and homogenous [31]. The corresponding EDX analysis of the SEM at pH13 solution of the elements by weight of the Alloy 1 was: 50.81% O, 8.15% Na, 1.07% Mg, 9.56% Al, 12.95% Si, 0.11% Cl, 0.46% Cr, 1.48% Fe, 1.68% Ni, 2.13% Cu, 11.56% Br and 0.04 % Zr. Correspondingly the elements of Alloy 2 at pH13 solution were: 47.40% O, 6.40% Na, 1.19% Mg, 15.45% Al, 12.08% Si, 0.13% Cl, 2.73% Fe, 0.85% Ni, 1.85% Cu, 11.71% Br and 0.20% Zr. The formations of higher aluminum oxide layer on the surfaces of the alloys save from the harm of the corrosion. The cases of lower corrosion rate EDX analysis confirmed that by showing higher level of oxidization.

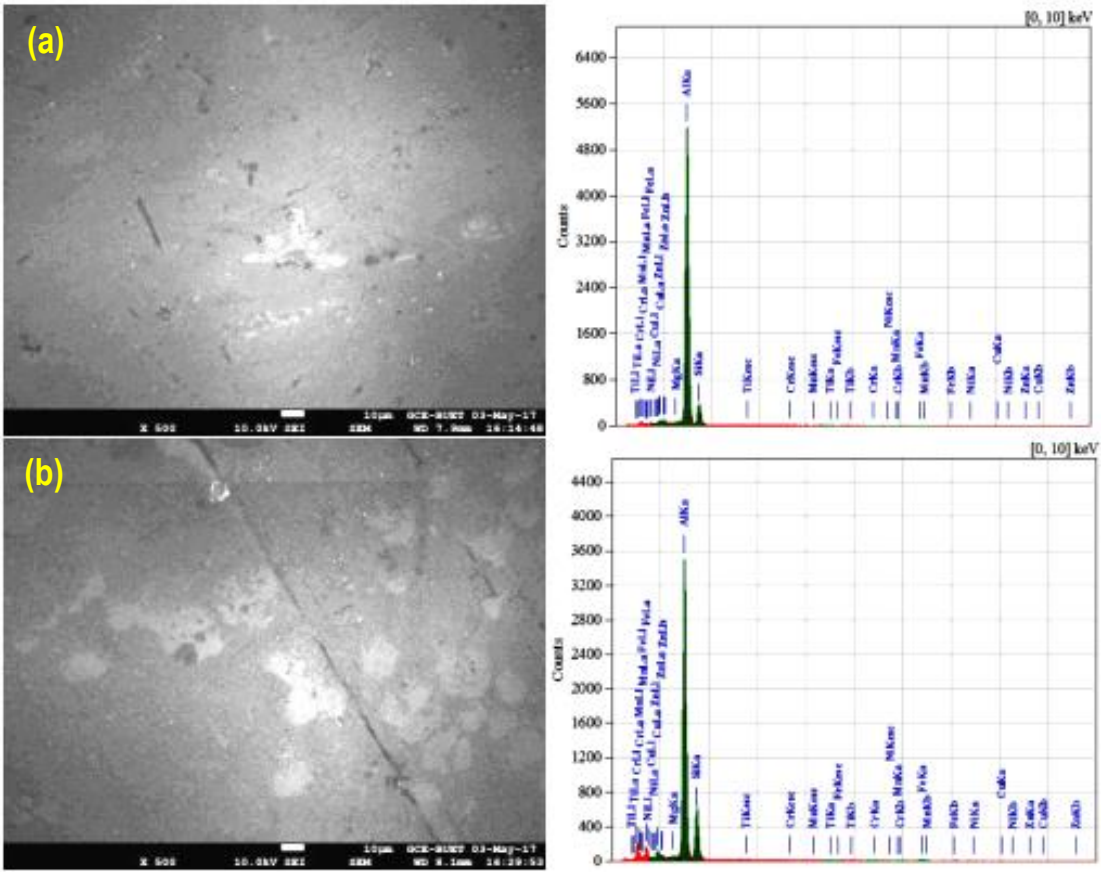

Fig. 9 – SEM images with EDX spectra analysis of the experimental (a) Alloy 1 and (b) Alloy 2 before corrosion

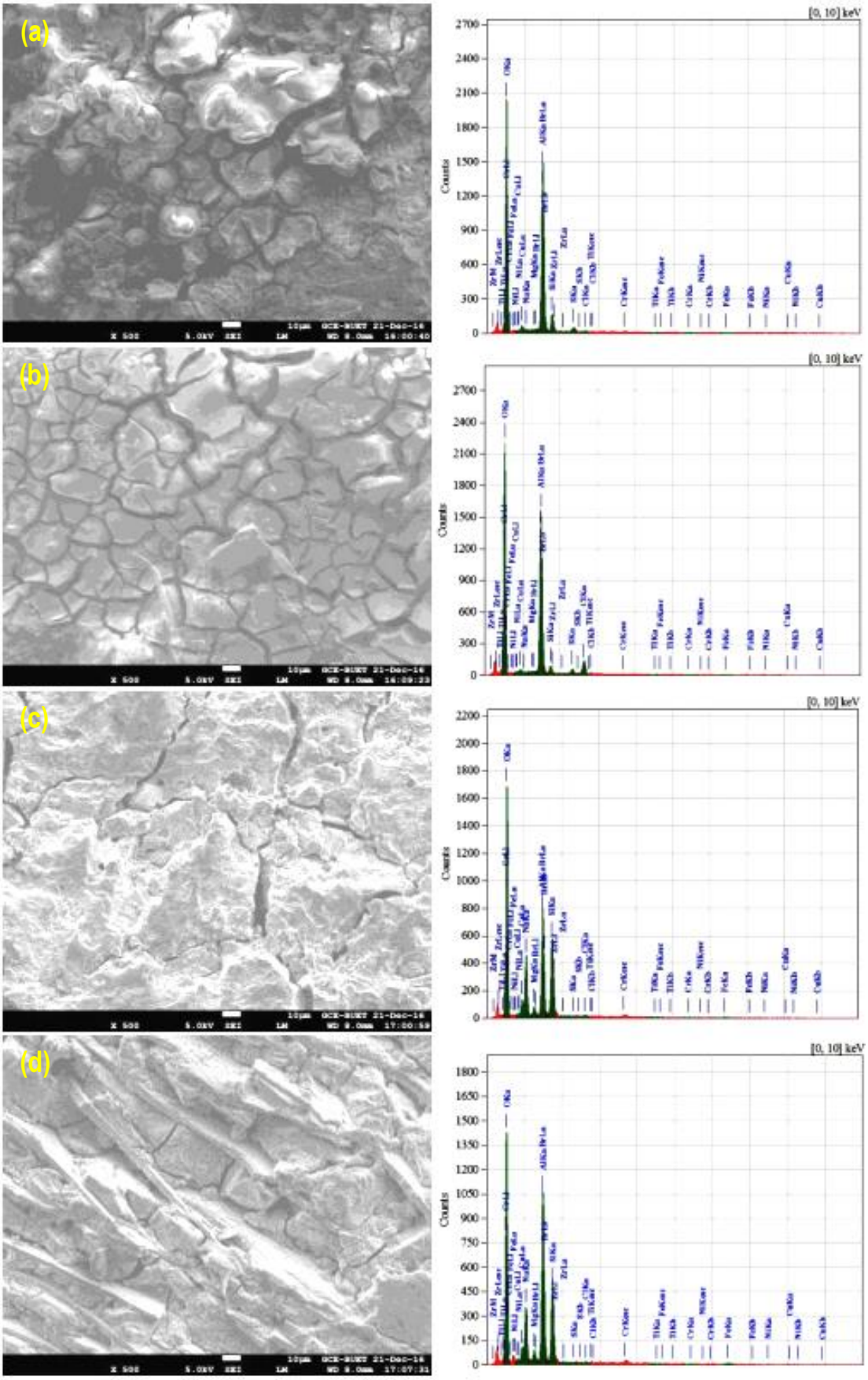

Fig. 10 – SEM images with EDX spectra analysis of (a) Alloy 1, (b) Alloy 2 after exposure in pH1 solution for 27 days and in pH13 solution (c) Alloy 1 and (d) Alloy 2 for the same days

4 Conclusions

From this literature review the following findings can be concise:

Iron added alloy shows the double aging peaks as the hyper-eutectic Al-Si automotive alloy and attain the higher strength ageing at 175°C for 4 hours. Formation of GP zones as well as the metastable phases be capable of strengthen the alloys and direct to the condition of peak aged.

Excessive Fe does not show addition ageing response but increases the overall hardness of the alloy lead to formation of different iron reach intermetallic like Al_3Fe, α-Al_8Fe_2Si, β-Al_5FeSi, δ-Al_4FeSi_2 and γ-Al_3FeSi during solidification.

Addition of Fe strongly degrades the tensile strength, elongation and fracture toughness related to mechanical properties of the alloy due to formation of needle-like intermetallic of β-Al_5FeSi phase in a plate-like morphology.

SEM microphotograph of Fe added alloy confirms higher volume fraction of the higher crack sensitive nature of coarser β-Al_5FeSi needles and primary Fe rich intermetallics. It could facilitate the initiation and the propagation of microcracks caused the poor wear resistance of these types of alloys.

Excessive alloying elements Fe degraded the corrosion behaviour of the Al-Si alloy at the acidic pH1 environment but improved it at the alkaline environment of pH13. Pores were produced through uniform degradation of the alloys surface immersed in acidic solution, but a thick film of oxide corrosion layer in black nature was formed on the surfaces of the alloys when affected in the alkaline solution.

Acknowledgements

For this study there no external funding was received.

REFERENCES

[1]- H. Ye, An overview of the development of Al-Si-Alloy based material for engine applications, Mater. Eng. Perform. 12(3) (2003) 288-297. doi:10.1361/105994903770343132

[2]- M.S. Kaiser, Effect of temperature on the corrosion behaviour of Al-12Si-1Mg automotive alloy in 3.5% NaCl solution, Int. J. Mater. Sci. Eng. 5(2) (2017) 87-94. doi:10.17706/ijmse.2017.5.2.87-94

[3]- O. Omodara, O.O. Daramola, J.L. Olajide, A.A. Adediran, O.S. Akintayo, B.O. Adewuyi, D.A. Desai, E.R Sadiku, Improved mechanical and wear characteristics of hypereutectic aluminium-Silicon alloy matrix composites and empirical modelling of the wear response, Cogent Eng. 7(1) (2020) 1-24. doi:10.1080/23311916.2020.1787010.

[4]- S. Liu, X. Zhang, H.L. Peng, X. Han, H.Y. Yang, T.T. Li, L. Zhu, S. Zhang, F. Qiu, Z.H. Bai, S.M. Chen, W. Zhou, Q.C. Jiang, In situ nanocrystals manipulate solidification behavior and microstructures of hypereutectic Al-Si alloys by Zr-based amorphous alloys, J. Mater. Res. Technol. 9(3) (2020) 4644-4654. doi:10.1016/j.jmrt.2020.02.091

[5]- M.S. Kaiser, M.R. Basher, A.S.W. Kurny, Effect of scandium on microstructure and mechanical properties of cast Al-Si-Mg alloy, J. Mater. Eng. Perform. 21(7) (2012) 1504-1508. doi:10.1007/s11665-011-0057-3

[6]- D. M. Maradiaga, O.V. Mishin, K. Engelbrecht, Thermal properties of selectively laser-melted AlSi10Mg products with different densities, J. Mater. Eng. Perform. 29(11) (2020) 7125-7130. doi:10.1007/s11665-020-05192-z

[7]- A.R. Farkoosh, M. Pekguleyuz, The effects of manganese on the T-phase and creep resistance in Al-Si-Cu-Mg-Ni alloys, Mater. Sci. Eng.-A. 582(2013) 248-256. doi:10.1016/j.msea.2013.06.030

[8]- M.S. Kaiser, Solution treatment effect on tensile, impact and fracture behaviour of trace Zr added Al-12Si-1Mg-1Cu piston Alloy, J. Inst. Eng. Ind.-D. 99(1) (2018) 109-114. doi:10.1007/s40033-017-0140-5

[9]- T.O. Mbuya, B.O. Odera, S.P. Nganga, Influence of iron on castability and properties of aluminium silicon alloys: literature review, Int. J. Cast Metal. Res. 16(5) (2003) 451-465. doi:10.1080/13640461.2003.11819622

[10]- D. Medvecka, L. Kucharikova and M. Uhricik, The Failure Degradation of Recycled Aluminium Alloys with High Content of β-Al5FeSi Intermetallic Phases." Defect and Diffusion Forum, 2020, vol. 403, pp. 97-102. doi:10.4028/www.scientific.net/ddf.403.97.

[11]- M.H. Abdelaziz, A.M. Samuel, H.W. Doty, S. Valtierra, F.H. Samuel, Effect of additives on the microstructure and tensile properties of Al–Si alloys, J. Mater. Res. Technol. 8(2) (2019) 2255-2268. doi:10.1016/j.jmrt.2019.03.003

[12]- M.S. Kaiser, Efffect of solution treatment on the age hardening behaviour of Al-12Si-1Mg-1Cu piston alloy with trace Zr addition, J. Cast. Mater. Eng. 2(2) (2018) 30-37. doi:10.7494/jcme.2018.2.2.30

[13]- F. Stadler, H. Antrekowitsch, W. Fragner, H. Kaufmann, P.J. Uggowitzer, Effect of main alloying elements on strength of Al–Si foundry alloys at elevated temperatures, Int. J. Cast Metal. Res. 25(4) (2012) 215-224. doi:10.1179/1743133612Y.0000000004

[14]- M.S. Kaiser, S.H. Sabbir, M. Rahman, M.S. Kabir, M. Al Nur, Heat treatment effect on the physical and mechanical properties of Fe, Ni and Cr added hyper-eutectic Al-Si automotive alloy, J. Chem. Technol. Metal. 55(2) (2020) 409-416.

[15]- M.S. Kaiser, S.H. Sabbirb, M.S. Kabir, M. Rahman, M. Al Nur, Study of mechanical and wear behaviour of hyper-eutectic Al-Si automotive alloy through Fe, Ni and Cr addition, J. Mater. Res. 21(4) (2018) 1-9. doi:10.1590/1980-5373-mr-2017-1096

[16]- M.S. Kaiser, M. Al Nur, Effect of Fe, Ni, and Cr on the corrosion behaviour of hyper-eutectic Al-Si automotive alloy under different pH conditions, J. Electrochem. Sci. Eng. 8(3) (2018) 241-253. doi:10.5599/jese.493

[17]- S. Kaiser, M.S. Kaiser, Influence of Aluminium and Zinc Additives on the Physical and Thermal Behaviour of Cast Copper, J. Sust. Struct. Mater. 3(1) (2020) 1-9. doi:10.26392/SSM.2020.03.01.001

[18]- D.L. Zhang, L. Zheng, The quench sensitivity of cast Al-7 wt pct Si-0.4 wt pct Mg alloy, Metal. Mater. Trans-A. 27(1996) 3983-3991. doi:10.1007/BF02595647.

[19]- K.T. Kashyap, S. Murali, K.S. Raman, K.S. Smurthy, Casting and heat treatment variables of Al–7Si–Mg alloy, Mater. Sci. Technol. 9(3) (1993) 189-204. doi:10.1179/mst.1993.9.3.189

[20]- S. Ji, F. Gao, D. Watson, Z. Fan, Effect of iron on the microstructure and mechanical property of Al– Mg–Si–Mn and Al–Mg–Si diecast alloys, Mater. Sci. Eng.-A. 564(2013) 130-139. doi:10.1016/j.msea.2012.11.095

[21]- S. Spigarelli, M. Cabibbo, E. Evangelista, J. Bidulska, A study of the hot formability of an Al-Cu-Mg-Zr alloy, J. Mater. Sci. 38(1) (2003) 81-88. doi:10.1023/A:1021161715742

[22]- S.G. Shabestari, The effect of iron and manganese on the formation of intermetallic compounds in aluminum–silicon alloys, Mater. Sci. Eng–A. 383(2) (2004) 289-298. doi:10.1016/S0921-5093(04)00832-9

[23]- M. Mahta, M. Emamy, A. Daman, A. Keyvani, J. Campbell, Precipitation of Fe rich intermetallics in Cr-and Co-modified A413 alloy, Int. J. Cast Met. Res. 18(2) (2005) 73-79. doi:10.1179/136404605225022928

[24]- R. Taghiabadi, H.M. Ghasemi, Dry sliding wear behaviour of hypoeutectic Al-Si alloys containing excess iron, Mater. Sci. Technol. 25(8) (2009) 1017-1022. doi:10.1179/174328408X302468

[25]- P.K. Rohatgi, Y. Liu, S. Ray, Friction and wear of metal-matrix composites. In: Blau PJ (ed) ASM Handbook, 1992, Volume 18: Friction, Lubrication, and Wear Technology. ASM International, Metals Park, Ohio, USA.

[26]- R. Taghiabadi, H.M. Ghasemi, S.G. Shabestari, Effect of iron-rich intermetallics on the sliding wear behavior of Al–Si alloys, Mater. Sci. Eng. 490(2008) 162-170. doi:10.1016/j.msea.2008.01.001

[27]- D. Prabhu, P. Rao, Corrosion Behaviour of 6063 Aluminum Alloy in Acidic and in Alkaline Media, Ar. J. Chem. 10(2017) 2234-2244. doi:10.1016/j.arabjc.2013.07.059

[28]- J.R. Galvele, Transport Processes and the Mechanism of Pitting of Metals, J. Electrochem. Soc. 123(1976) 464-474.

[29]- B.A. Shaw, T.L. Fritz, G.D. Davis, W.C. Moshier, Influence of tungsten on the pitting of aluminum films, J. Electrochem. Soc. 137(4) (1990) 1317-1318.

[30]- A.M. Samuel, H.W Doty, S. Valtierra and F.H. Samuel, Beta Al_5FeSi phase platelets-porosity formation relationship in A319.2 type alloys, Int. J. Metalcast. 12(1) (2018) 55-70. doi:10.1007/s40962-017-0136-9

[31]- M. Al Nur, M.S. Kaiser, Int. J. Mech. Mater. Eng. 11(11) (2017) 1736-1740. doi:10.5281/zenodo.1132623